JOURNAL OF GEOPHYSICAL RESEARCH, VOL. 100, NO. D2, PAGES 3173–3180, FEBRUARY 20, 1995

Outgoing longwave radiation biases and their impacts on empirical orthogonal function modes of interannual variability in the tropics

Mary T. Kayano
Instituto Nacional de Pesquisas Espaciais, São José dos Campos, Brazil

Vernon E. Kousky and John E. Janowiak
National Meteorological Center, Climate Analysis Center, Washington, D. C.

Abstract. The effects of different equator-crossing times on the outgoing longwave radiation (OLR) data record are examined. A simple procedure proposed by Kousky and Kayano (1994) is used to reduce these effects. Large-scale interannual modes of OLR within the tropics are determined by performing empirical orthogonal function analyses on OLR anomalies and on bias-corrected OLR anomalies. Both analyses result in two physically meaningful leading modes, which describe different large-scale anomalous features of the OLR related to the southern oscillation. A mode related to changes in the satellite observing system is found only in the analysis for the uncorrected OLR anomalies. Evidence is presented indicating that estimates of the mean daily OLR are affected by changes in the equator-crossing times due either to the replacement of satellites or to long-term drifts from the orbital plane during the lifetime of individual satellites.

1. Introduction

Outgoing longwave radiation (OLR) data have been used in many studies to investigate interannual (IA) variability of deep tropical convection [e.g., *Liebmann and Hartmann*, 1982; *Rasmusson and Arkin*, 1985]. The OLR data set has a resolution of 2.5° in latitude and longitude and is derived from radiance that is measured twice a day from the NOAA operational polar-orbiting satellites (NOAA SR series from June 1974 to February 1978, and TIROS N series from January 1979 to the present). Since the beginning of the record, there have been several changes in satellites, their times of observation, instrumentation, and in the algorithms used to estimate the OLR, which have caused biases in the OLR record. Studies to reduce this bias have considered two kinds of changes: (1) The changes in instrumentation and in the computational procedures used to estimate the OLR, and (2) the changes in equator-crossing times [*Gruber and Krueger*, 1984].

The NOAA SR series satellites used the scanning radiometer (SR), while the TIROS N series satellites used the advanced very high resolution radiometer (AVHRR) to estimate OLR. The width of the window channel of the radiometers, from which the measurements have been taken, has also changed several times. The infrared window channel between 10.5 and 12.5 microns was used for the NOAA SR series, and a channel extending from 10.5 to 11.5 microns was used for TIROS N and NOAA 6 [*Gruber and Krueger*, 1984]. Two infrared channels were available for NOAA 7, NOAA 9, and NOAA 11. The window extending from 11.5 to 12.5 microns was chosen to estimate OLR from these satellites [*Kidwell*, 1991].

The original computational procedure to derive the OLR from the radiometric measurements, proposed by *Wark et al.* [1962], has been revised several times [*Abel and Gruber*, 1979; *Ellingson and Ferraro*, 1983; *Ohring et al.*, 1984; *Ellingson et al.*, 1989]. *Ohring et al.* [1984] empirically determined the coefficients of the OLR estimation equation by using regression analysis of the data from NIMBUS 7. This scheme to estimate OLR began to be operationally used on March 1, 1983 [*Janowiak et al.*, 1985]. The previous OLR data were corrected by the equations derived by *Gruber and Krueger* [1984].

Temporal biases in the observations due to the diurnal cycle of OLR have been reduced by averaging day and night observations [*Gruber and Krueger*, 1984; *Janowiak et al.*, 1985]. Another source of inhomogeneity in OLR data record has been attributed to differences in the equator-crossing times among the various satellites [*Chang and Kousky*, 1987; *Chelliah and Arkin*, 1992; *Gadgil et al.*, 1992]. *Chelliah and Arkin* [1992] found that one of the leading modes of a principal component analysis, based on the monthly OLR anomalies over the tropics for the period from June 1974 to March 1989, is related to this inhomogeneity. *Gadgil et al.* [1992] presented evidence that systematically higher OLR fluxes in the tropics, estimated from the NOAA SR series, are related to changes in the satellite observing system.

Also, the equator-crossing times of some individual satellites have not remained constant during their lifetimes. Errors in orbital insertion and atmospheric drag cause orbital departures from exact sun-synchronous orbit, and the equator-crossing time drifts slowly during the lifetime of the satellite. *Chelliah and Arkin* [1992] suggested that the satel-

Paper number 94JD02949.
0148-0227/95/94JD-02949$05.00

lite drift could contribute to variations in the OLR estimates during the lifetime of each satellite.

The objective of this paper is to address further OLR biases related to changes in equator-crossing times. We provide evidence that these changes, due to either satellite replacement or to a long-term drift of the orbital plane during the lifetime of each individual satellite, introduce inhomogeneities in the OLR data record. Since OLR has been a key parameter in many studies on IA variability, we also investigate the impacts that these inhomogeneities have on the principal modes of IA OLR variability.

2. Data and Methodology

The data set used consists of 5-day nonoverlapping (pentad) means of OLR, for the period from January 1979 through December 1988, which is available at the Climate Analysis Center, Washington, D. C. For this period, the computational procedures to estimate the OLR and the instrumentation are quite homogeneous.

The OLR anomalies are calculated with respect to a 10-year (1979–1988) climatology, which was computed using the method described by *Kousky* [1988]. First the 10-year average OLR is computed for each pentad and then the 73 pentads (representing the entire year) are smoothed using a 5-pentad running mean filter. Time series of OLR anomalies are selected on a staggered grid in the belt between 40°N and 40°S, with a resolution of 10° in latitude and longitude. Thus each field consists of 324 gridpoints. In order to remove the inhomogeneities due to changes in the equator-crossing times, we applied the bias correction procedure described by *Kousky and Kayano* [1994]. This procedure consists of removing the mean OLR anomaly patterns from the data for each of the periods corresponding to when the TIROS N, NOAA 6, and NOAA 7, 9, and 11 satellites were operational, respectively. The resulting time series will be referred to hereafter as bias-corrected time series.

Interannual timescale fluctuations are isolated by temporally filtering the time series with a low-pass Lanczos filter consisting of 97 weights and having a cutoff frequency of 0.0275 pentad^{-1}, which are the only inputs required by the method. The filter response is expressed as a Fourier series so that the weights become the Fourier coefficients. The weights for the low-pass filter used in the present paper are calculated using the following equation

$$w_k = \left[\frac{\sin(2\pi * 0.0275k)}{\pi k}\right] \frac{\sin(\pi k/n)}{\pi k/n}, \qquad (1)$$

where n is 48, and k is $-n, \cdots, 0, \cdots n$. For a detailed description of the Lanczos filter, the reader is referred to work by *Duchon* [1979], and for a description of the low-pass Lanczos filter, as used here, the reader is referred to *Kousky and Kayano* [1994]. Application of this filter results in the loss of 96 pentads (48 at the beginning and 48 at the end of the record). Thus the total number of pentads is reduced from 730 to 634.

We used the estimated mean temperature over interior Australia, derived from the Japanese geostationary meteorological satellite (GMS) geostationary satellite, to assist in diagnosing the temporal sampling effects of the polar-orbiting satellite data. These data were obtained from the Global Precipitation Climatology Project (GPCP) [*Janowiak and Arkin*, 1991] and are available on a 2.5° latitude and longitude grid. Infrared data are collected from GMS by the Japanese Meteorological Agency for the GPCP, and pentad means are constructed for each 3-hour daily period (00, 03, $\cdots$, 21 UTC). In addition to mean temperature, histograms of pixel brightness temperatures within each grid box are saved in the GPCP record. The histograms are stratified into 16 temperature classes that are at intervals of 5 K (except 10 K near the extremes), and the warmest class is reserved for pixels with brightness temperatures exceeding 270 K.

From these data, we constructed 12 grand monthly means over the period 1988 through 1992 of 3-hour mean temperature. That is, for each month, the 5-year (1988–1992) mean of temperature for each 2.5° latitude and longitude region was computed for each 3-hour period (00 UTC, 03 UTC, etc.). Since pentads do not generally fit evenly into months, the pseudo monthly means were constructed from the pentad means by weighting the contribution of each pentad by the number of days that a pentad falls into the month being considered. For example, pentad 7 (January 31 through February 4) spans over a month boundary, so a "weight" of 1 is given to this pentad to construct the January mean, and a weight of 4 is given when computing the February mean. All pentads that fall completely within a month receive a weight of 5. The weighted accumulations are then divided by the sum of all weights to yield a pseudo monthly average.

To ensure that only surface temperatures are used, we use the histogram data to screen out cloudy cases. This is accomplished by using only those temperatures for cases in which 1% or less of the pixels within a grid box were colder than 270 K during a pentad. These temperatures represent the window temperatures and are used to estimate the OLR by applying the operational procedure previously introduced by *Gruber and Krueger* [1984].

The principal method of analysis in this paper is empirical orthogonal function (EOF) analysis. The statistical method of EOF analysis has been extensively used in climate studies [e.g., *Kutzbach*, 1967; *Hardy and Walton*, 1978; *Horel and Wallace*, 1981]. The reader is referred to work by *Kutzbach* [1967] for a comprehensive description of this method. The IA patterns of OLR anomalies were determined by performing an unrotated EOF analysis on the filtered time series and on the bias-corrected filtered time series. The EOF analysis is based on the correlation matrix. In this paper the principal components are referred to as the amplitude time series and the elements of a particular eigenvector or mode are referred to as loadings. The loading at each gridpoint represents the linear correlation between the time series of the original data (used in the EOF analysis) at that gridpoint and the amplitude time series corresponding to a particular mode.

The results are discussed in the next section. The OLR patterns obtained for the EOF analysis on filtered time series are presented in section 3.1., and those based on bias-corrected filtered time series are given in section 3.2. Effects of the changes of the equator-crossing time on the OLR data record are discussed in section 3.3.

3. Results

3.1. EOF Analysis for Uncorrected OLR Time Series

The first three unrotated patterns for uncorrected OLR are shown in Figures 1a–1c. The first IA mode explains 15% of

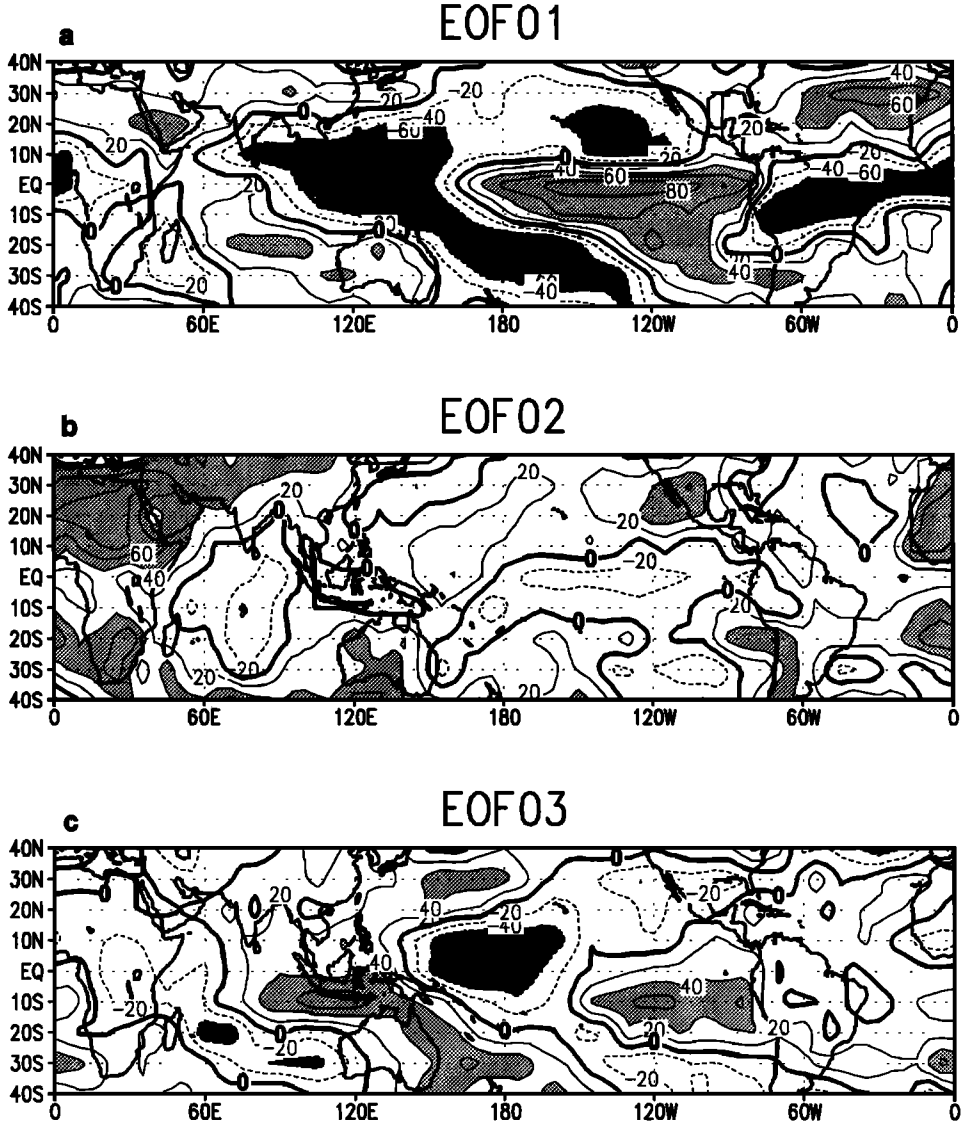

Figure 1. The first three interannual EOF modes for OLR anomalies, computed for the period 1979–1988. The loadings, which vary from −1 to 1, are multiplied by 100. The contour interval is 20. Values less (greater) than −40 (40) are indicated by dark (light) shading.

the total IA variance. This mode (Figure 1a) describes large-scale OLR features associated with extremes in the southern oscillation (SO), as indicated by its amplitude time series (Figure 2a). For positive (negative) amplitudes, positive (negative) OLR loadings are located over the tropical Pacific, the subtropical North Atlantic, and subtropical South America. Negative (positive) OLR loadings are located over Indonesia, the eastern Indian Ocean, the subtropical North Pacific and southwestern South Pacific, the Amazon Basin and the adjacent equatorial Atlantic. Negative amplitudes for this mode are found during the 1982–1983 and 1986–1987 El Niño–Southern Oscillation (ENSO) episodes (warm phase of the SO), while positive amplitudes are found during the relatively cold periods of 1981 and 1984–1985. This mode is essentially the same as the first mode obtained by *Chelliah and Arkin* [1992] based on monthly means for the period June 1974–March 1989.

The second IA OLR mode (Figure 1b) explains 10% of the total IA variance. This mode is very similar to the third mode found by *Chelliah and Arkin* [1992], which they related to changes in satellite equator-crossing times. For positive (negative) amplitudes, desert areas are dominated by positive (negative) OLR loadings (Figure 1b). As indicated in Table 1 and Figure 2b, negative amplitudes are dominant during the period when NOAA 6 was the operational satellite (equator-crossing times near sunrise/sunset), and positive amplitudes dominate the period when TIROS N, NOAA 7, 9, and 11 were the operational satellites (late night/midafternoon equator-crossing times). These features imply that this mode reflects the difference in estimates of the mean daily OLR produced by sampling the diurnal cycle at different times. The mean daily estimates would be the same, if the diurnal cycle were a perfect harmonic. However, as will be shown in section 3.3., the diurnal cycle shows considerable asymmetry that leads to differences in the estimates of daily mean OLR for the various equator-crossing times. The negative amplitudes during early 1985 (Figure 2b) coincide with the replacement of NOAA 7 by NOAA 9 (see Table 1).

The third IA mode explains 8.0% of the total IA variance. This mode (Figure 1c) seems to be linked to the SO but

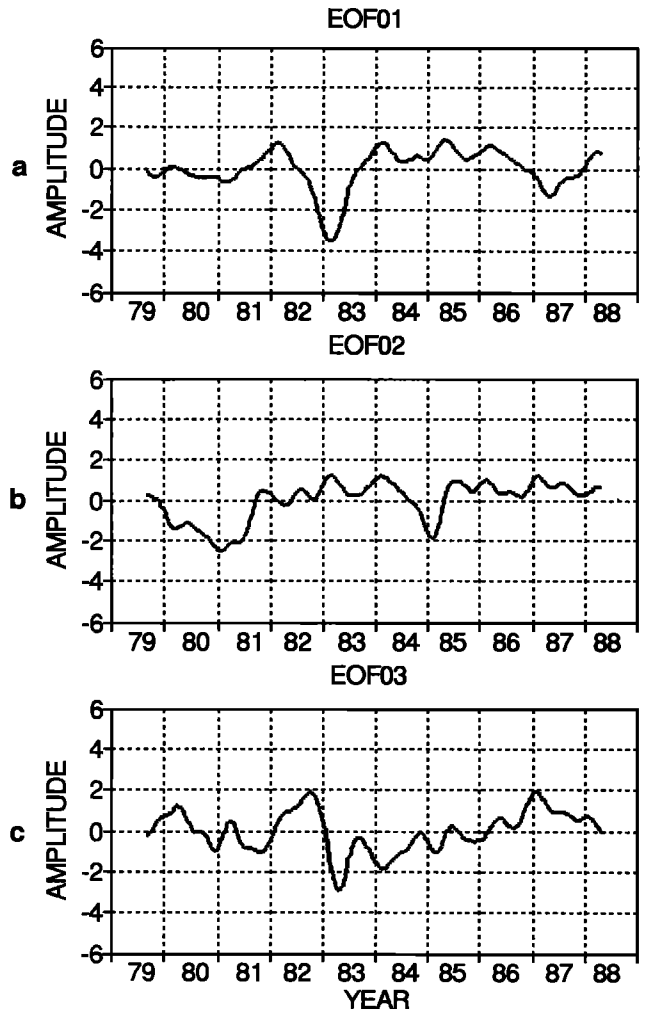

Figure 2. Amplitude time series for the first three interannual modes for the OLR patterns shown in Figure 1.

describes aspects of the OLR variations related to the SO different from those of the first IA mode. The amplitude time series of the third mode (Figure 2c) indicates that it tends to emphasize the early stage of negative extremes (warm episodes) of the SO. For positive amplitudes, positive OLR loadings are located over Indonesia, the eastern Indian Ocean, the subtropics in the western Pacific, and the eastern tropical Pacific, and negative OLR loadings are located over the tropical western and central Pacific (centered slightly west of the dateline). Positive amplitudes are found during warm episode onset years of 1982 and 1986 and also throughout 1987. The negative extreme amplitude of this mode occurred in early 1983, at the height of the 1982–1983 warm episode, when enhanced convection was observed over the eastern equatorial Pacific and over Indonesia. Negative amplitudes were also featured during the weak cold episode period of 1984, when convection was enhanced primarily over Indonesia [*Quiroz*, 1984; *Wagner*, 1985].

Of the three leading modes, the second mode relates to the bias in the OLR data record due to changes in the equator-crossing times. We propose a simple procedure to reduce this bias. Table 1 gives the nominal equator-crossing times of the ascending/descending node (northbound/southbound) in local solar time (LST) for the TIROS N series. The January 1979–August 1992 period includes three periods with different equator-crossing times (Table 1). To minimize the effect of sampling at different times of the day, the mean pattern of OLR anomalies (Figure 3), computed with respect to the 1979–1988 base period, is removed for each of these periods. Unfortunately, this procedure also removes real interannual variability for regions not affected by the differences in the equator-crossing times. The pattern corresponding to the period when NOAA 6 was the operational satellite (Figure 3b) shows negative values over low-latitude continental desert regions. A nearly opposite pattern is found for the period corresponding to the NOAA 7, 9, and 11 satellites (Figure 3c). These features are consistent with those shown in the second IA mode (Figure 1b), which reflects the biases that result from sampling the diurnal cycle at different times. In the next section we compute the principal modes for the bias-corrected data in order to determine if the biases have any effect on the first and third modes.

3.2. EOF Analysis on Bias-Corrected OLR Time Series

The EOF analysis based on bias-corrected OLR anomalies does not reproduce the mode related to the changes in the satellite observing systems. The modes related to the southern oscillation are the two leading modes in the new analysis and together they explain 24% of the total IA variance. The IA OLR patterns for these modes are shown in Figure 4, and their amplitude time series are shown in Figure 5. A comparison between these figures and those corresponding to the first and third modes of the previous EOF analysis indicates that these modes are basically the same in both analyses. Also, the percentage of the total IA variance explained by these two modes is almost the same in both analyses. These results show that the bias in the original OLR data record has been eliminated and the SO signal has been preserved by using the bias correction procedure. Furthermore, the bias contained in the original OLR anomalies does not affect the IA modes which are related to physically meaningful phenomena.

3.3. Effects of the Changes in the Equator Crossing Times on OLR

The amplitude time series of the second mode presented in section 3.1. is very smooth, since it has been obtained from an EOF analysis of low-pass filtered OLR anomalies. A time series which retains the IA and shorter timescale fluctuations is constructed by calculating the scalar product between the original pentad OLR anomalies for the period 1979–1992 and the second mode loadings obtained in section 3.1. This time series (Figure 6) shows high-frequency fluctuations superim-

Table 1. Equator-Crossing Times (Local Standard Time, LST) and Periods of OLR Observations for the Operational Polar-Orbiting Satellites During the Period 1979–1992

Satellite	Equator-crossing Time, LST	Period
TIROS N	0330–1530LST	Jan. 1979–Jan. 1980
NOAA 6	0730–1930LST	Feb. 1980–Aug. 1981
NOAA 7	0230–1430LST	Sept. 1981–Feb. 1985
NOAA 9	0220–1420LST	March 1985–Nov. 1988
NOAA 11	0140–1340LST	Nov. 1988–Aug. 1992

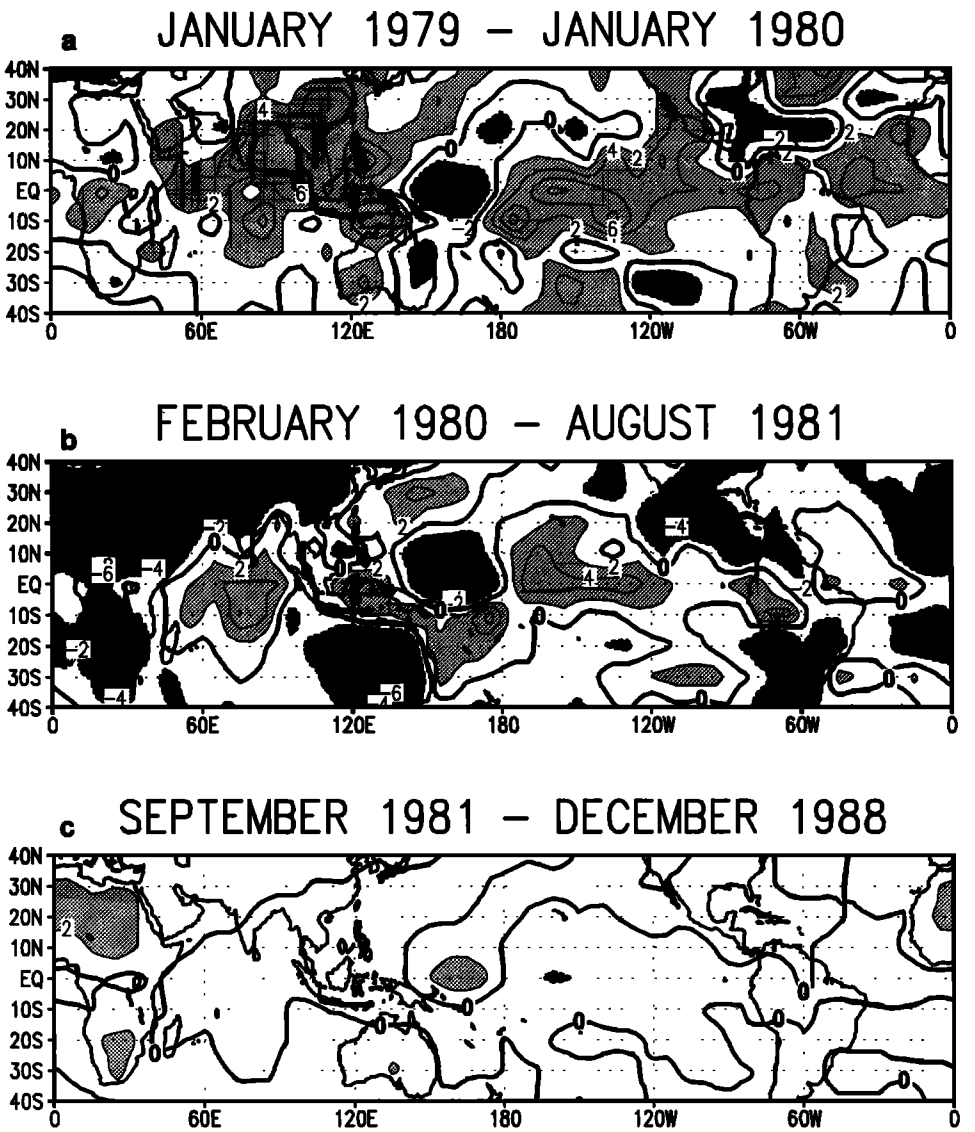

Figure 3. Mean patterns of OLR anomalies for a) January 1979–January 1980, (b) February 1980–August 1981, and (c) September 1981–December 1988. The contour interval is 2 W m^{-2}. Values less (greater) than −2 (2) are indicated by dark (light) shading.

posed on IA variations related to changes in the equator-crossing times.

Similar to Figure 2a, negative amplitudes (Figure 6) are found during the operation of the NOAA 6 satellite, and mostly positive amplitudes are found during the period of operation of the TIROS N, NOAA 7, 9, and 11 satellites. The abrupt changes during the beginning of 1980, late in 1981, and early in 1985 correspond to periods when the operational satellites were being replaced. Except for NOAA 6, the operational satellites during the period 1979–1992 had "at launch" equator-crossing times of post midnight and mid-afternoon. During its lifetime, each satellite departs slowly from its original orbital plane, resulting in a drift of the equator-crossing time. The equator-crossing times for the NOAA 7, 9, and 11 satellites during their lifetimes are shown in Figure 7. Thus even for these satellites with nearly the same equator-crossing times "at launch," their drift resulted in a change in the equator-crossing time of 1–3 hours at the time of their replacement.

A more careful examination of Figure 6 indicates a downward trend in the amplitudes throughout the periods corresponding to the operation of each satellite. A possible explanation for this is that the drift in the equator-crossing times results in a shift of the daytime observations with respect to the peak in the diurnal cycle of surface temperature, thus reducing the estimate of the daily mean OLR. To explore this possibility further, we calculated the mean annual estimated OLR at 3-hour intervals from the GMS geostationary satellite for an arid region in Australia (23.75°S–28.75°S and 128.75°E–133.75°E), where the diurnal cycle is most pronounced. The maximum OLR flux occurs at 1200 LST, and the minimum is observed at 0600 LST (Figure 8). The day plus night average estimated OLR values are 294 W m^{-2}, 276 W m^{-2}, 282 W m^{-2}, and 297 W m^{-2} for the observing times at 1500–0300 LST, 1800–0600 LST, 2100–0900 LST and 0000–1200 LST, respectively. Comparing Figures 7 and 8, it is clear that the drift in the equator-crossing times (from approximately 1500 to nearly 1800 LST)

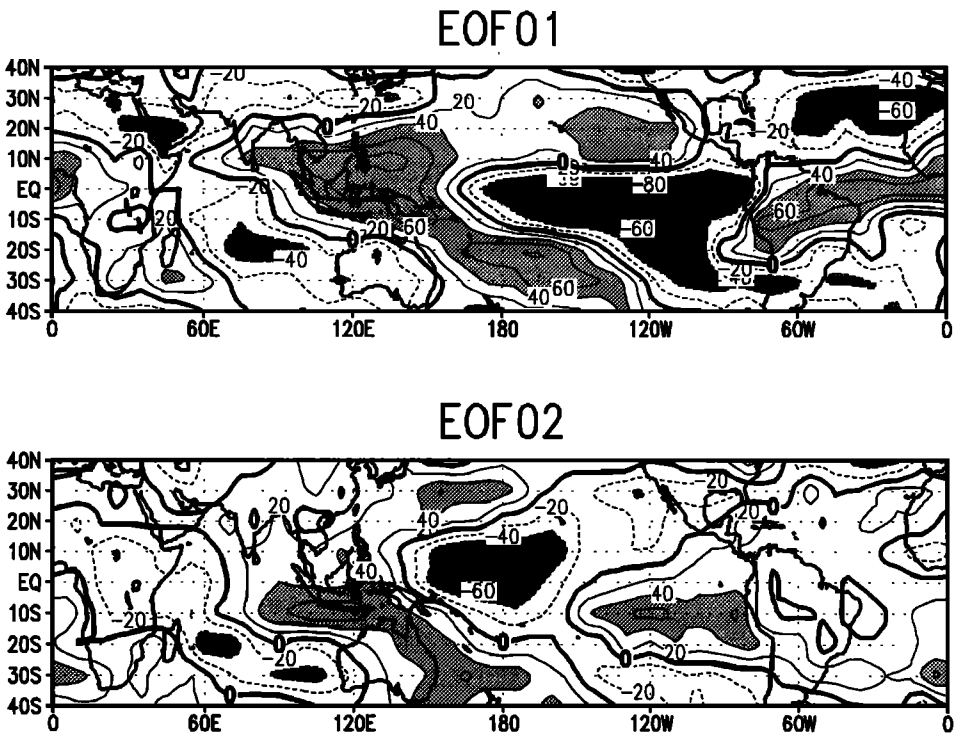

Figure 4. The first two interannual EOF modes for bias-corrected OLR anomalies, computed for the period 1979–1988. Display is the same as that in Figure 1.

for the NOAA 7, 9, and 11 satellites results in a decrease in the estimated daytime OLR, which results in a reduction of the daily mean averaged OLR.

It is also important to note that the effects of the drift in equator-crossing time are dependent primarily on the time of the daytime observation. For example, a 1-hour shift in the equator-crossing time during early afternoon (1200 LST to 1500 LST) results in a decrease of the estimated OLR by approximately 3 W m^{-2}, while a 1-hour shift during late afternoon (1500 LST to 1800 LST) results in a decrease of up to 18 W m^{-2}. Thus different equator crossing times due to either replacement of satellites or long-term drift from the orbital plane during the lifetime of single satellites may result in considerable bias in the OLR data, especially for arid and semiarid regions where a strong diurnal cycle in surface temperature exists.

4. Summary and Conclusions

The effects of the changes in the equator-crossing times on the OLR, derived from radiometric measurements taken from the TIROS N polar-orbiting satellites, have been investigated. Large-scale interannual (IA) variations of the OLR within the tropics have been determined by performing EOF analyses on uncorrected OLR anomalies and on bias-corrected OLR anomalies.

The EOF analysis performed on uncorrected OLR anomalies yielded two physically meaningful leading (first and third) modes, which describe different large-scale anomalous features of the OLR related to the southern oscillation (SO). Another leading (second) mode is related to "nonphysical" OLR variations attributed to changes in the satellite observing system. This mode reflects basically the strong diurnal cycle of the surface temperature over desert regions, which results from sampling the diurnal cycle at different times of the day. Daily mean OLR values based on nighttime/midafternoon (TIROS N, NOAA 7, 9, and 11) observing times are higher than those based on near sunrise/near

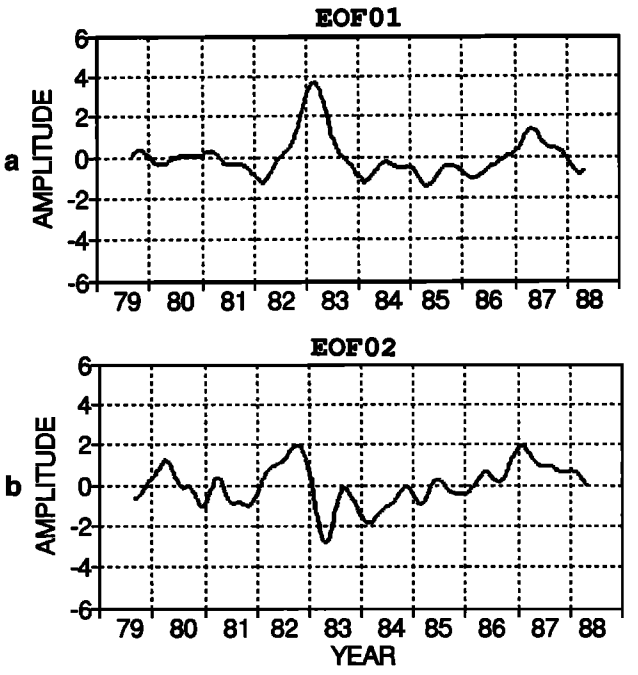

Figure 5. Amplitude time series for the first two interannual modes for the OLR patterns shown in Figure 4.

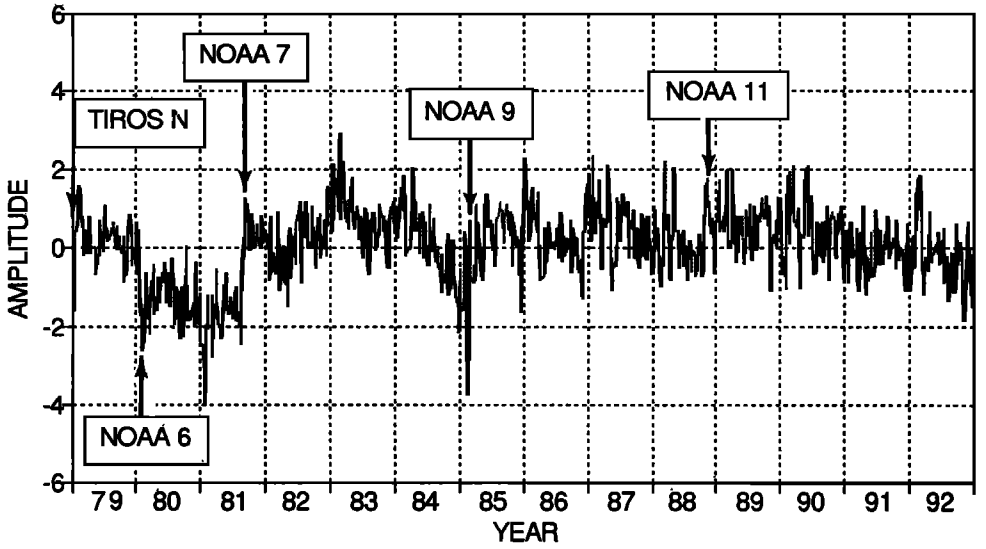

Figure 6. Amplitude time series obtained by computing the scalar product between the original unfiltered anomaly fields and mode 2 in Figure 1.

sunset (NOAA 6) observing times, resulting in significant differences in the estimated mean daily OLR. These differences or biases are sufficiently large that they appear as a leading interannual mode.

The first two leading modes obtained by performing EOF analysis on the bias-corrected OLR anomalies are related to the SO. This analysis does not reproduce the "nonphysical" mode related to the changes in the satellite observing system. The percentage of the total IA variance explained by the two SO-related modes is nearly the same in both analyses. Thus the bias in the original OLR data record has been eliminated and the SO signal has been preserved by using the bias correction procedure. Furthermore, the bias contained in the original OLR anomalies does not affect the IA modes related to physically meaningful phenomena.

Evidence has been presented indicating that changes in the equator-crossing times, due either to the replacement of satellites or to a long-term drift from the orbital plane during the lifetime of a satellite, affect the OLR data record. In addition, evidence has also been presented that demonstrates how a drift in the equator-crossing time results in a gradual reduction of the daily mean OLR values during the lifetime of a satellite. Although the biases resulting from shifts in the equator-crossing times are sufficient to cause

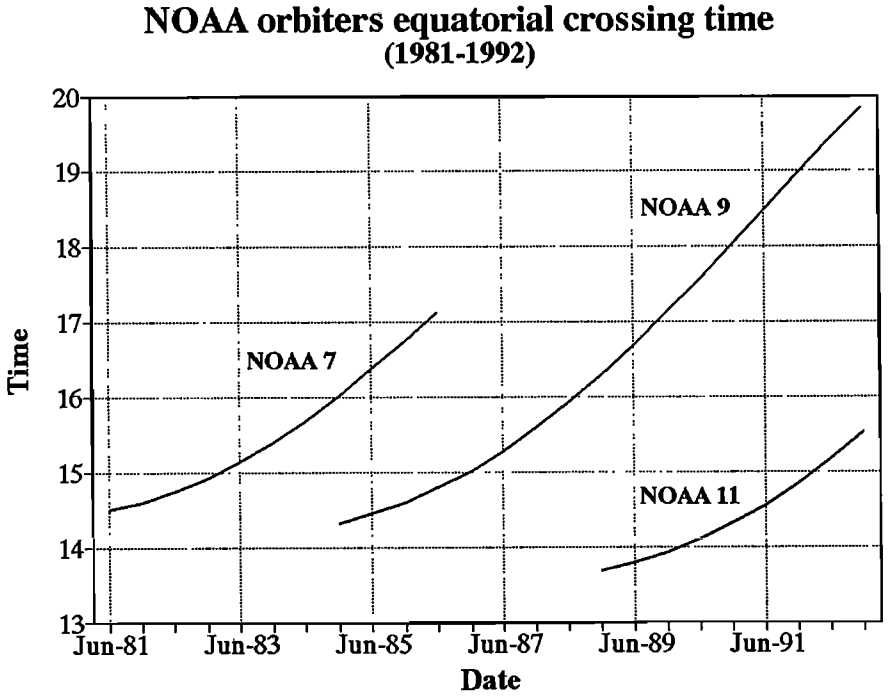

Figure 7. Equator-crossing times for NOAA 7, NOAA 9, and NOAA 11 satellites during their lifetimes. Courtesy of N. Rao from the National Environmental Satellite, Data and Information Service (NESDIS).

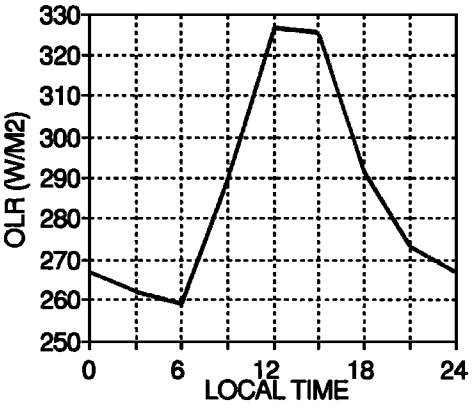

Figure 8. Annual mean diurnal cycle of OLR, estimated from the mean temperature derived from the Japanese "GMS" geostationary satellite, for a region (23.75°S–28.75°S and 128.75°E–133.75°E) in central Australia.

unwanted interannual variability and trends in the OLR data record, the use of EOF analysis in our example effectively separated the physically meaningful modes from the non-physical mode related to the biases. Thus the principal modes of IA variability can be obtained without correcting the OLR data for the biases introduced due to satellite replacement of drift in the equator-crossing times. However, we suggest that the bias correction be made prior to computing indices based on areal averages of the OLR.

Acknowledgments. We are grateful to Nagaraja Rao for providing us with Figure 7. We also wish to thank the reviewers for their suggestions and comments.

References

Abel, P., and A. Gruber, An improved model for the calculation of longwave flux at 11 μm, *Tech. Rep., NESS 106*, 24 pp., Natl. Oceanic Atmos. Admin., Silver Spring, Md., 1979.

Chang, F. C., and V. E. Kousky, An observational study of interaction between large scale tropical cumulus convection and the equatorial circulation anomalies, *Proc. Annu. Clim. Diagnostics Workshop, 12th*, 256–265, 1987.

Chelliah, M., and P. A. Arkin, Large-scale interannual variability of monthly outgoing longwave radiation anomalies over the global tropics, *J. Clim., 5*, 371–389, 1992.

Duchon, C. E., Lanczos filtering in one and two dimensions, *J. Appl. Meteorol., 18*, 1016–1022, 1979.

Ellingson, R. G., and R. R. Ferraro, Jr., An examination of a technique for estimating longwave radiation budget from satellite radiance observations, *J. Clim. Appl. Meteorol., 22*, 1416–1423, 1983.

Ellingson, R. G., D. J. Yanuk, and A. Gruber, Effects of the choice of meteorological data on a radiation model simulation of the NOAA technique for estimating outgoing longwave radiation from satellite radiance observations, *J. Clim., 2*, 761–765, 1989.

Gadgil, S., A. Guruprasad, and J. Srinivasan, Systematic bias in the NOAA outgoing longwave radiation dataset?, *J. Clim., 5*, 867–875, 1992.

Gruber, A., and A. F. Krueger, The status of the NOAA outgoing longwave radiation data set, *Bull. Am. Meteorol. Soc., 65*, 958–962, 1984.

Hardy, D. M., and J. J. Walton, Principal components analysis of vector wind measurements, *J. Appl. Meteorol., 17*, 1153–1162, 1978.

Horel, J. D., and J. M. Wallace, Planetary scale atmospheric phenomena associated with the Southern Oscillation, *Mon. Weather Rev., 109*, 813–829, 1981.

Janowiak, J. E., and P. A. Arkin, Rainfall variations in the tropics during 1986–1989, as estimated from observations of cloud-top temperature, *J. Geophys. Res., 96*, 3359–3373, 1991.

Janowiak, J. E., A. F. Krueger, and P. A. Arkin, Atlas of outgoing longwave radiation derived from NOAA satellite data, *NOAA Atlas 6*, 44 pp., Natl. Oceanic Atmos. Admin., Silver Spring, Md., 1985.

Kidwell, K. B., NOAA Polar Orbiter Data (TIROS N, NOAA 6, NOAA 7, NOAA 8, NOAA 9, NOAA 10, NOAA 11, and NOAA 12) *Users Guide*, 206 pp., U.S. Dep. of Commer., NOAA/NESDIS, Washington, D. C., 1991.

Kousky, V. E., Pentad outgoing longwave radiation climatology for the South American Sector, *Rev. Bras. Meteorol., 3*, 217–231, 1988.

Kousky, V. E., and M. T. Kayano, Principal modes of outgoing longwave radiation and 250-mb circulation for the South American sector, *J. Clim., 7*, 1131–1143, 1994.

Kutzbach, J. E., Empirical eigenvectors of sea-level pressure, surface temperature and precipitation complexes over North America, *J. Appl. Meteorol., 6*, 791–812, 1967.

Liebmann, B., and D. L. Hartmann, Interannual variations of outgoing IR associated with tropical circulation changes during 1974–78, *J. Atmos. Sci., 39*, 1153–1162, 1982.

Ohring, G., A. Gruber, and R. G. Ellingson, Satellite determinations of the relationship between total longwave radiation flux and infrared window radiance, *J. Clim. Appl. Meteorol., 23*, 416–425, 1984.

Quiroz, R. S., The climate of the 1983–84 winter—A season of strong blocking and severe cold in North America, *Mon. Weather Rev., 112*, 1894–1912, 1984.

Rasmusson, E. M., and P. A. Arkin, Interannual climate variability associated with the El Niño/Southern Oscillation, in *Coupled-Ocean Atmosphere Models*, edited by J. C. J. Nihoul, pp. 289–302, Elsevier, New York, 1985.

Wagner, A. J., The climate of spring 1984—An unusually cold and stormy season over much of the United States, *Mon. Weather Rev., 113*, 149–169, 1985.

Wark, D. Q., G. Yamamoto, and J. Lienesch, Methods of estimating infrared flux and surface temperature from meteorological satellites, *J. Atmos. Sci., 19*, 369–384, 1962.

J. E. Janowiak and V. E. Kousky, Diagnostics Branch Climate Analysis Center, NOAA NWS, National Meteorological Center, Washington, DC 20233. (e-mail:wdszvk@sun1.noaa.gov)

M. T. Kayano, Instituto Nacional de Pesquisas Espaciais, CP 515, 12.227 900, São José dos Campos, SP, Brazil.

(Received December 29, 1994; revised September 21, 1994; accepted November 4, 1994.)